Physical modelling of the piano: An investigation into the effect of string stiffness on the hammer-string interaction

CHARALAMPOS SAITIS

Physical modelling of the piano: An investigation into the effect of string stiffness on the hammer-string interaction

A DISSERTATION

submitted to Queen's University Belfast
in partial fulfillment of the requirements
for the degree of

Master of Arts in Sonic Arts

CHARALAMPOS SAITIS

Sonic **A**rts **R**esearch **C**entre
School of Music and Sonic Arts
Belfast, Northern Ireland, UK

Abstract

The stiff string wave equation has four solutions, two of which are related to the string stiffness. In the case of digital waveguide modelling these are neglected [Bensa 2003]. Current research suggests that all four travelling waves should be considered, at least at the neighbourhood of the excitation point [Ducasse 2005]. This dissertation investigates the effect of omitting string stiffness in the context of sound synthesis of the piano by physical modelling. A stiff, lossy string with a spatially distributed hammer force excitation is implemented using both a finite-difference time-domain scheme and a digital waveguide model. The two models are designed so as to have the exact same features but for the two stiffness-related solutions. The numerical experiments study the contact force signal over time for different initial velocity values. The resulting sounds are also discussed. The results generally confirm that the two fast-decaying waves cannot be ignored during simulation. The effect of string stiffness becomes more audible in the low register of the piano as the initial velocity increases, whereas in the high-frequency region results are more ambiguous.

Contents

List of symbols

X	spatial step
T	time step
m	spatial index
n	time index
f_s	sampling frequency
M	number of string segments
$y(x,t)$	string displacement
$\eta(t)$	hammer displacement
$\xi(t)$	hammer felt compression
ρ	linear density of the string
c	wave velocity
$F_H(t)$	hammer force
$g(x,x_0)$	spatial window
λ	Courant number
L	string length
M_S	string total mass
T_e	string tension
b_1	air damping coefficient
b_2	string internal friction coefficient
ϵ	string stiffness parameter
κ	string stiffness coefficient
M_H	hammer mass
p	hammer felt stiffness exponent
b_H	fluid damping coefficient
K	hammer felt stiffness
x_0	excitation point
$a = x_0/L$	relative striking position

f_1	fundamental frequency
f_0	fundamental frequency of the ideal string
f_n	modal frequency
s	complex frequency
ω	angular frequency
k	wavenumber
E	Young's modulus
S	cross-section area of the string
r	radius of the string
v	velocity
F	force (general)
R	characteristic impedance of the string
$r(t)$	relaxation function
σ	hysteresis constant
τ	relaxation constant
R_l	left boundary impedance
R_b	bridge impedance
F_b	string force on the bridge
$H_B(k,\omega)$	frequency response of the right boundary filter
$H_L(k,\omega)$	frequency response of the left boundary filter
r_L	reflectance of the left boundary
r_B	reflectance of the bridge
ζ_l	left end normalized impedance
ζ_b	bridge normalized impedance

Chapter 1

Introduction

> 'Every time I try something,' the Prince said, 'I gain a little.'
> –Bruce Chatwin, *In Patagonia.*

Musical instruments are complex mechanisms. How do they work? What makes a trumpet sound like a trumpet? What distinguishes a good instrument maker from a *very* good one? To provide answers, acoustics has been trying to understand the fundamentals of sound production for centuries. Most recently, the study of musical instruments acoustics in the context of digital sound synthesis has made significant contributions towards more detailed understanding of their sounding mechanisms.

Starting from the examination of the physical principles of a musical instrument, a system of—often partial but not always—differential equations that describe the acoustical and mechanical behaviour of the instrument is derived. The methods for discrete time-domain simulation of such spatially distributed acoustic systems are referred to as *physical modelling*. Sound synthesis by physical modelling is also known as *physics-based sound synthesis*. The objective is nicely summarized by Adrien in [Adrien 1991]: "[...] to represent a general sound-producing instrument as a collection of vibrating structures, responding to external demands, interacting together and feeding

the radiated field."

The physics-based approach to sound synthesis is advantageous and indeed sophisticated compared to other methods. The use of abstract algorithms (frequency modulation, wavetable synthesis), pre-recorded samples (sampling synthesis, granular synthesis), and spectral information (additive synthesis, spectral modelling) forms techniques that eventually model the signal itself rather than the mechanism that produced it. Moreover, the physics-based approach succeeds in implementing the interaction between the instrument and the instrumentalist. The reason is the direct relation of most of the model parameters to the "real-world" instrument characteristics, e.g. the length of the string, or the diameter of the reed. The following example[1] illustrates another important benefit: The basic difference between the Greek bouzouki and its Irish descendant is the shape of the body[2]: by altering the corresponding parameters one can switch from one model to the other. Also, modifying the parameters allows investigation of specific features of the instrument by listening to the resulting sound. However, this shows that physical models are limited in that they refer to a specific instrument, or family of instruments. They are also computationally demanding. In some cases the use of digital signal processing techniques, e.g. digital waveguide modelling (see Chapter 3) has helped reducing the implementation cost significantly, allowing efficient synthesis [Smith 1992]. This dissertation considers

[1]Inspired by a similar example given in [Bank 2000].

[2]The Greek bouzouki is a stringed instrument with a pear-shaped body, a member of the lutes family. It was introduced into Irish traditional music in 1966 by Johnny Moynihan. It soon became popular and an Irish-music-specific version was developed, which has a wider body with flat back and straight sides. In 1970 English luthier Peter Abnett built an instrument with a four-course Greek bouzouki neck and a shallow-arched, three-piece back. He called it Irish bouzouki. A detailed reference can be found on `http://www.irishbouzouki.com/`.

physical modelling of the piano, investigating the effect of string stiffness on the hammer-string interaction.

The one-dimensional wave equation for the transverse displacement of a stiff and lossy string has four solutions, two weakly attenuated and two fast-decaying travelling waves [Ducasse 2005]. In the case of digital waveguide modelling the latter are omitted [Bensa 2003]. However, these solutions are related to the stiffness of the string. When the string is excited—by a piano hammer in this case—"*the bend is rounded appreciably by the stiffness of the string*" [Fletcher 1998]. Ducasse notices that it is the presence of the fast-decaying waves that restrains a sharp bend. In his paper [Ducasse 2005], he argues that the stiffness-related solutions cannot be neglected, but rather be carefully considered when the string interacts with the hammer, i.e. at the neighbourhood of the excitation point, or the bridge. He agrees that the fast-decaying waves can be ignored in other parts of the string, which have no sources and are long enough. Accordingly, Ducasse concludes that the digital waveguide model presented in [Bensa 2003] has to be complemented at the excitation point, and points out the need for further investigation in the context of sound synthesis. No such study has been attempted so far, at least not that the author of this dissertation is aware of.

The purpose of this dissertation is to study and implement the effect of (omitting) string stiffness in the context of sound synthesis of the piano by physical modelling. If the stiffness-related waves are taken into account when implementing the hammer-string interaction, will the quality of the synthesized sound be improved noticeably? To investigate this, a stiff and lossy string with scalar impedance and a spatially distributed hammer force

excitation using both a finite-difference time-domain scheme and a digital waveguide model was numerically simulated. The two models are designed so as to have the exact same characteristics but for the two stiffness-related solutions. The contact force signal over time for different initial velocity values, as well as the resulting sounds are examined.

Chapter 2 introduces the basic acoustical properties of the piano. Chapter 3 presents the principles of piano modelling considered for the present purposes. Sections 3.1 and 3.2 provide the necessary background on the finite-difference time-domain method and the digital waveguide modelling respectively. Section 3.3 focuses on the hammer-string interaction, presenting the underlined physics, and the various modelling approaches. Chapter 4 provides the design and numerical simulation of the two models. Chapter 5 presents the experiments and discusses the results. Finally, Chapter 6 summarizes, and concludes.

Chapter 2

Acoustic behaviour of the piano

The piano is one of the most popular musical instruments. It belongs to the family of stringed keyboard instruments. Considering an alternative classification, it is often referred to as a struck string instrument. From Bach and the *Well-Tempered Clavier* to Ligeti and the *Piano Études*, and from Beethoven's *Piano Sonata in C-sharp minor "Moonlight"* to Stockhausen's *Klavierstück VIII*, the piano has its own very history.

The modern piano descends directly from the harpsichord. In 1709, Bartolomeo Cristofori, an Italian maker of musical instruments, solved the fundamental problem of the hammer-string contact and built the first piano. He understood that if the hammer remained in contact with the string after the strike (as in the clavichord), then the sound would be damped. Moreover, the hammer should return to its rest position without bouncing violently, and the action should allow rapid note repetition. Hofstadter begins his famous book [Hofstadter 2000] with a historical reference on Cristoforis invention:

> Frederick [the Great, King of Prussia] was one of the first patrons of the arts to recognise the virtues of the newly developed "piano-forte" ("soft-loud"). The piano had been developed in the

> first half of the eighteenth century as a modification of the harpsichord. The problem with the harpsichord was that pieces could only be played at a rather uniform loudness—there was no way to strike one note more loudly than its neighbours. The "soft-loud", as its name implies, provided a remedy to this problem. From Italy [...] the soft-loud idea had spread widely. Gottfried Silbermann, the foremost German organ builder of the day, was endeavouring to make a "perfect" piano-forte. Undoubtedly King Frederick was the greatest supporter of his efforts—it is said that the King owned as many as fifteen Silbermann pianos!

Cristofori called his new instrument *"gravicembalo col piano et forte"*. Of course many changes and improvements were necessary before reaching the modern form of the piano. The evolution of the instrument saw the development of two distinct types, the grand piano and the upright piano. The latter was developed in the middle of the nineteenth century and its action differs from that of the first [Fletcher 1998]. For the purposes of this work, the grand piano is considered. However, much of the discussion that follows accounts for the upright piano as well. Also, only the piano strings and hammers are considered in the present investigation. Therefore, detailed description of other parts of the instrument is omitted.

2.1 Piano design and action

The piano is compiled mainly by the keyboard, the action, the strings, the soundboard, and the frame. One end of the strings is close to the keyboard, connected on the pin block through the tuning pins. From there they extend

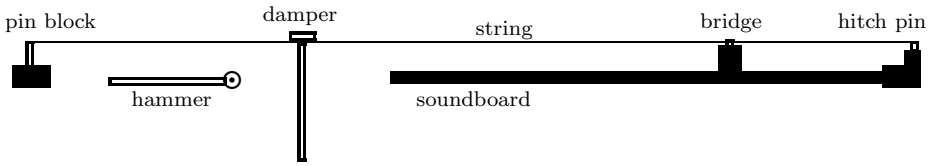

Figure 2.1: A simplified diagram of the piano mechanism.

across the bridge to the hitch-pin rail. The bridge acts as the transmitter of the string vibration to the soundboard. The striking mechanism or action is directly attached to the keyboard. Figure 2.1 provides a simplified representation of the overall structure. To produce sound, the pianist presses a key down, starting thus the action off. This causes the hammer to strike the string. The vibrations of the string are then passed on to the soundboard via the bridge. Finally, the sound is produced by the vibrating soundboard.

The action is complex and precise. When the key is pressed down, it sets the hammer to motion towards the string. When halfway down, the back end of the key causes the damper to be raised from the string. Continuing, the hammer strikes the string and rebounds. Immediately it is caught by the backcheck and is not released until after the key is released. That way rapid repetition of single notes is allowed without the key having to return to its rest position. A more detailed description of the piano design and action can be found in [Benade 1976] and [Fletcher 1998]. It is worth mentioning that the piano action is a lever system in that the hammer has greater velocity than the key [Hall 1990].

2.2 Piano strings and inharmonicity

The strings lie at the heart of the instrument and its mechanism. They transform part of the kinetic energy of the hammer into vibrational energy, which they store in their normal modes of vibration, while the rest disperses due to internal friction. The stored vibrational energy eventually determines the resulting sound, as described above.

The strings of the piano are made of high-strength steel wire. For efficiency of sound production they are stretched to 30-60% of their yield strength [Fletcher 1998]. The treble strings are solid wire whereas the bass strings have a solid core wound with one or two layers of copper wire. That way the mass of the bass strings is increased without affecting likewise the string stiffness, and thus inharmonicity. Greater mass is necessary for the low-frequency strings, otherwise their length, which is inversely proportional to the fundamental frequency, would have to be too long.

The coupling between the strings, the bridge, and the soundboard is a critical aspect of piano strings. To improve the coupling without increasing the mass of the string—and hence inharmonicity—multiple strings for each note are used. These are referred to as coupled strings. A set of three coupled strings, which is usually the case in all but the lowest two octaves, is called a *tricord* [Fletcher 1998]. Often, two coupled strings are used for the higher bass notes. Coupled strings are, however, slightly mistuned, introducing beating and two-stage decay, two typical characteristics of piano timbre [Bank 2000]. A thorough reference on coupled piano strings can be found in [Weinreich 1977].

Inharmonicity is a result of the string stiffness. The modal frequencies of a stiff string with pinned ends are:

$$f_n = n f_0 \left(1 + n^2 B\right)^{1/2} , \qquad B = \frac{\pi^2 E S r^2}{T_e L^2}$$

where n refers to the partial, f_0 is the fundamental frequency of the ideal string (i.e. the same string without stiffness), T_e and L are the tension and length of the string respectively, E is the Young's modulus, S is the cross-section area of the string, and r is the radius of guration of the cross-section [Fletcher 1998].

Inharmonicity is another typical characteristic of piano timbre. Early simulations have shown that otherwise a piano would sound "unnatural" [Reinholdt 1987]. It is more perceptually discernible at low pitches, even though the previous equation implies the opposite. This can be explained considering psychoacoustics: the limit of perceiving inharmonicity increases with frequency [Järveläinen 1999]. Furthermore, inharmonicity affects the tuning of the piano, being responsible for stretching the lower and upper octaves below and above the equal tempered pitches respectively [Conklin 1996b].

Longitudinal vibration of the piano strings affects the piano timbre significantly. A comprehensive presentation can be found in [Conklin 1996b].

2.3 Piano hammers and string excitation

Hammers are an integral part of the piano action, influencing the timbral character of the instrument significantly. Piano hammers are made of hardwood cores of graduated sizes, covered by one or two layers of wool felt of

varying thickness that increases from treble to bass. Felt allows adjusting the hammer hardness during the process of voicing. Moreover it exhibits dynamic hardness that varies with hammer velocity, hence affecting the spectrum at various dynamic levels. When the velocity is high, the hammer felt is effectively harder, and hence causes better excitation of the high-frequency modes in the string. Therefore, the spectrum becomes richer in high-frequency components [Conklin 1996a, Fletcher 1998]. Accordingly, the hammer felt can be considered as a hardening spring, that is a nonlinear spring, the stiffness of which increases with compression [Fletcher 1998]. Hence, the force due to the felt F_H can be described by the following power law:

$$F_H = K\xi^p \,, \tag{2.1}$$

where K is the stiffness, ξ is the felt compression, and p is the stiffness exponent, i.e. it describes how much stiffness changes with force. By choosing proper values for K and p, the hammer-string interaction can be modelled—this will be discussed further in the next Chapter. Moreover, force-compression measurements suggest hysteresis characteristics for the interaction [Fletcher 1998].

The excitation of the piano string by the hammer is a nonlinear phenomenon. After initiation of the action, the hammer strikes the string. Due to its considerable mass, the hammer remains in contact with the string for several instants, during which reflected pulses return from both ends of the string and interact with the hammer in a rather complicated way. The hammer is eventually thrown clear of the string, and the latter is left vibrating

freely in its normal modes. The duration of the hammer-string contact depends on their mass ratio [Chaigne 1994b, Fletcher 1998]: a heavier hammer may remain longer in contact, or make multiple contacts. In the middle register, a contact time equal to the half period of the tone is found to account for effective string excitation [Hall 1988]. In the upper register the contact duration is longer, whereas in the lower register the hammer is thrown back from the string by the first arriving reflected pulses.

The position of the striking point on the string plays an important role on its excitation as well. The modes of vibration for which nodes exist near to the striking point will be excited less effectively [Conklin 1996a]. This results in a comb filtering effect in the spectrum [Bank 2000].

The hammer-string interaction is one of the most important aspects of piano physics. Accordingly, it has been the subject of considerable research in physics-based sound synthesis of the piano. The next Chapter concentrates on physical modelling methods for piano strings considering the hammer-string interaction. Further elements of piano acoustics can be found in [Benade 1976] and [Fletcher 1998].

Chapter 3

Elements of piano modelling

This chapter considers piano string modelling while implementing the hammer-string interaction. The three most popular physics-based string modelling techniques are the finite-difference method, modal synthesis and most recently the functional transformation method, and digital waveguide modelling. Sections 3.1 and 3.2 provide the theoretical and mathematical background of the first and the latter respectively, as these are the methods used in the present investigation. A comprehensive review of the various approaches to physics-based discrete time-domain simulation of musical instruments can be found in [Välimäki 2006]. Section 3.3 focuses on the case of the hammer-string interaction. Section 3.4 summarizes while drawing some conclusions on string modelling.

3.1 Finite differences

The first physics-based simulation of a vibrating string was introduced by Hiller and Ruiz in 1971 [Hiller 1971a, Hiller 1971b], where they applied the *finite-difference time-domain* (FDTD) method. This method originates from computational electrodynamics [Taflove 1995]. It was introduced by Yee in

1966 with regards to direct time-domain solutions of Maxwells equations [Yee 1966]. Since then the modelling capabilities of the method have been exploited in various field of engineering. In physics-based sound synthesis it is more often referred to as the *finite-difference method* (FDM). In reality the FDM does not refer to a single method but rather to a family of numerous FDTD schemes. They all function in the space-time grid using "neighbouring points", however the approach to defining the operators each time differs. An extensive analysis of FDTD schemes for the wave equation can be found in [Bilbao 2004a]. The advantage of this method is obvious: the resulting explicit scheme is obtained directly from the equations that describe the physics of the instrument. Accordingly, the synthesis algorithm will contain the instruments physical attributes. Furthermore, the technique straightforward implements two- and three-dimensional structures. The major drawback is the high computational complexity and cost, particularly met in multi-dimensional models.

3.1.1 The ideal string

Consider a uniform string of length L with linear density ρ stretched to a tension T_e that vibrates. The one-dimensional scalar wave equation for the transverse displacement $y = y(x,t)$ of the string is then [Fletcher 1998]

$$\frac{\partial^2 y}{\partial t^2} = \frac{T_e}{\rho}\frac{\partial^2 y}{\partial x^2}.$$

By substituting the wave velocity $c = \sqrt{T_e/\rho}$, the more familiar form

$$\frac{\partial^2 y}{\partial t^2} = c^2 \frac{\partial^2 y}{\partial x^2} \tag{3.1}$$

is obtained. The analytical derivation of the wave equation can be found in [Morse 1948] and [Fletcher 1998]. The next step is to approximate the derivatives by finite differences. These are obtained by considering the space-time grid $x_m = mX,\ t_n = nT,\ X$ being the spatial sampling interval and T the temporal sampling interval, and using the Taylor series expansions of $y(x, t_n)$ about the space point x_m to the space points $x_m + X$ and $x_m - X$ respectively [Taflove 1995]:

$$\begin{aligned} y(x_m + X)|_{t_n} &= y|_{x_m,t_n} + X\frac{\partial y}{\partial x}\bigg|_{x_m,t_n} + \frac{X^2}{2}\frac{\partial^2 y}{\partial x^2}\bigg|_{x_m,t_n} + \frac{X^3}{6}\frac{\partial^3 y}{\partial x^3}\bigg|_{x_m,t_n} \\ &\quad + \frac{X^4}{24}\frac{\partial^4 y}{\partial x^4}\bigg|_{\xi_1,t_n}, \quad \xi_1 \in (x_m, x_m + X) \end{aligned} \tag{3.2a}$$

$$\begin{aligned} y(x_m - X)|_{t_n} &= y|_{x_m,t_n} - X\frac{\partial y}{\partial x}\bigg|_{x_m,t_n} + \frac{X^2}{2}\frac{\partial^2 y}{\partial x^2}\bigg|_{x_m,t_n} - \frac{X^3}{6}\frac{\partial^3 y}{\partial x^3}\bigg|_{x_m,t_n} \\ &\quad + \frac{X^4}{24}\frac{\partial^4 y}{\partial x^4}\bigg|_{\xi_2,t_n}, \quad \xi_2 \in (x_m - X, x_m)\ . \end{aligned} \tag{3.2b}$$

The last terms in both (3.2a) and (3.2b) are the remainder terms—often referred to as the error terms. Adding the two expansions gives

$$y(x_m + X)|_{t_n} + y(x_m - X)|_{t_n} = 2y|_{x_m,t_n} + X^2 \frac{\partial^2 y}{\partial x^2}\bigg|_{x_m,t_n} + \frac{X^4}{12}\frac{\partial^4 y}{\partial x^4}\bigg|_{\xi_3,t_n},$$

where $\xi_3 \in (x_m - X, x_m + X)$ according to the mean value theorem. Omitting the error terms and adopting the notation $y_m^n = y(x_m, t_n)$ results in

$$\frac{\partial^2 y}{\partial x^2}\bigg|_{m,n} = \frac{y_{m+1}^n - 2y_m^n + y_{m-1}^n}{X^2}. \tag{3.3}$$

This is known as the centered finite-difference approximation to the second-order partial space derivative of y. Repeating with respect to time, the centered finite-difference approximation to the second-order partial time derivative of y is obtained:

$$\frac{\partial^2 y}{\partial t^2}\bigg|_{m,n} = \frac{y_m^{n+1} - 2y_m^n + y_m^{n-1}}{T^2}. \tag{3.4}$$

Substituting the approximation expressions (3.3) and (3.4) into (3.1) and solving for y_m^{n+1} gives

$$y_m^{n+1} = a_{10}(y_{m+1}^n + y_{m-1}^n) + a_{11}y_m^n - y_m^{n-1}\,, \tag{3.5}$$

where

$$\begin{aligned} a_{10} &= \lambda^2 \\ a_{11} &= 2 - 2\lambda^2 \end{aligned}$$

are convenient coefficients and $\lambda = cT/X$ is the Courant number. This is an explicit scheme in that it computes the next time-step $n+1$ from the

known previous steps n and $n-1$. Infinitely rigid boundary conditions are modelled by setting $y_0^n = 0 = y_M^n$ for all n, where $m = 0, 1, 2, \ldots, M$, M being the number of segments, i.e. $L = MX$.

3.1.2 Von Neumann stability analysis

The explicit FDTD scheme described in (3.5) has to be computationally stable. That is the time-step T must be bounded so that no growing solutions exist [Thomas 1995]. *Von Neumann analysis* provides a classical approach to numerical stability. It applies frequency-domain techniques in that it investigates an FDTD scheme for solutions of the form

$$y_m^n = e^{snT+jkmX} \ , \tag{3.6}$$

where s is the complex frequency, j the imaginary unit, and k the wavenumber [Bilbao 2008]. Substituting such a solution into (3.5) yields the following characteristic equation, also known as the *amplification equation*:

$$z + 2(2\lambda^2 sin^2(kx/2) - 1) + z^{-1} = 0, \tag{3.7}$$

where $z = e^{sT}$ is the so called *amplification factor*. The necessary and sufficient condition for (3.5) to be stable is

$$|z| \leq 1 \quad \forall\, k \ ,$$

where z represents the roots of (3.7) [Thomas 1995, Taflove 1995, Bilbao 2008].

After some algebra it can be shown that this is equivalent to

$$\lambda^2 sin^2(kh/2) \leq 1 \quad \forall\, k\ ,$$

which yields

$$\lambda \leq 1.$$

This is known as the Courant-Friedrichs-Lewy condition [Thomas 1995]. Finally, to obtain an upper bound for the time-step:

$$T \leq \frac{X}{c}.$$

For a given sampling rate f_s, an upper bound for the spatial step can be obtained:

$$X \leq cT\ , \quad T = 1/f_s\ .$$

Considering the equality case $T = X/c$ above Eq. (3.5) becomes

$$y_m^{n+1} = y_{m+1}^n + y_{m-1}^n - y_m^{n-1}. \tag{3.8}$$

Here the wave travels exactly one spatial sampling interval in one temporal sampling interval. Interestingly enough, Eq. (3.8) is an *exact* solution to the wave equation (3.1) in that there is no numerical dispersion. Hence this case is often referred to as the *magic time-step* [Taflove 1995]. Moreover,

Eq. (3.8) is actually equivalent to the travelling-wave solution of (3.1). This is discussed further considering digital waveguide modelling.

3.1.3 The stiff and lossy string

In real vibrating strings there are frequency-dependent losses caused by air damping and internal friction, as well as dispersion due to the string stiffness. To model dispersion, the wave equation (3.1) is extended by adding a stiffness-related term:

$$\frac{\partial^2 y}{\partial t^2} = c^2 \frac{\partial^2 y}{\partial x^2} - \kappa^2 \frac{\partial^4 y}{\partial x^4}, \tag{3.9}$$

where κ is a string stiffness coefficient. This fourth-order spatial derivative originates from modelling the bending waves in bars [Fletcher 1998]. For frequency dependent losses Hiller and Ruiz [Hiller 1971a, Hiller 1971b] and later Chaigne and Askenfelt [Chaigne 1994a, Chaigne 1994b] suggested to add the following terms to the righthand side of (3.9):

$$-2b_1 \frac{\partial y}{\partial t} + 2b_2 \frac{\partial^3 y}{\partial t^3},$$

with b_1, b_2 being damping coefficients. However, the resulting equation has growing solutions for certain values of b_2 [Bensa 2003]. To overcome this a slightly altered term is proposed in the same paper:

$$-2b_1 \frac{\partial y}{\partial t} + 2b_2 \frac{\partial^3 y}{\partial x^2 \partial t}. \tag{3.10}$$

Adding (3.10) to (3.9) gives the wave equation for the stiff and lossy string:

$$\frac{\partial^2 y}{\partial t^2} = c^2 \frac{\partial^2 y}{\partial x^2} - \kappa^2 \frac{\partial^4 y}{\partial x^4} - 2b_1 \frac{\partial y}{\partial t} + 2b_2 \frac{\partial^3 y}{\partial x^2 \partial t} \ . \tag{3.11}$$

To discretize the first-order temporal derivative and the fourth-order spatial derivative the following centered finite-difference operators are used:

$$\left.\frac{\partial y}{\partial t}\right|_{m,n} = \frac{y_m^{n+1} - y_m^{n-1}}{2T} \ , \tag{3.12}$$

$$\left.\frac{\partial^4 y}{\partial x^4}\right|_{m,n} = \frac{y_{m+2}^n - 4y_{m+1}^n + 6y_m^n - 4y_{m-1}^n + y_{m-2}^n}{X^4} \ . \tag{3.13}$$

In the case of the second term in (3.10), however, the use of a centered finite-difference operator leads to an implicit scheme, which raises the computational cost. Instead, a so called *backward* finite-difference operator is applied with respect to time t [Bensa 2003]:

$$\left.\frac{\partial^3 y}{\partial x^2 \partial t}\right|_{m,n} = \left.\frac{\partial\left(\frac{\partial^2 y}{\partial x^2}\right)}{\partial t}\right|_{m,n} = \frac{\left.\frac{\partial^2 y}{\partial x^2}\right|_{m,n} - \left.\frac{\partial^2 y}{\partial x^2}\right|_{m,n-1}}{T}$$

$$= \frac{y_{m+1}^n - 2y_m^n + y_{m-1}^n - y_{m+1}^{n-1} + 2y_m^{n-1} - y_{m-1}^{n-1}}{X^2 T} \ . \tag{3.14}$$

Substituting the operators (3.12), (3.13), and (3.14) together with (3.3) and (3.4) into (3.11) and solving for y_m^{n+1} gives

$$\begin{aligned} y_m^{n+1} &= a_1(y_{m+2}^n + y_{m-2}^n) + a_2(y_{m+1}^n + y_{m-1}^n) + a_3 y_m^n \\ &\quad + a_4 y_m^{n-1} + a_5(y_{m+1}^{n-1} + y_{m-1}^{n-1}) \; . \end{aligned} \tag{3.15}$$

The coefficients a_i are defined as follows:

$$a_1 = \frac{-\lambda^2\mu}{1 + b_1 T} \tag{3.16a}$$

$$a_2 = \frac{\lambda^2 + 4\lambda^2\mu + \nu}{1 + b_1 T} \tag{3.16b}$$

$$a_3 = \frac{2 - 2\lambda^2 - 6\lambda^2\mu - 2\nu}{1 + b_1 T} \tag{3.16c}$$

$$a_4 = \frac{-1 + b_1 T + 2\nu}{1 + b_1 T} \tag{3.16d}$$

$$a_5 = \frac{-\nu}{1 + b_1 T} \; , \tag{3.16e}$$

where $\mu = \kappa^2/c^2X^2$ and $\nu = 2b_2T/X^2$ are convenient variables. This FDTD scheme is again explicit as it computes the next time-step $n+1$ from the known previous steps n and $n-1$. Boundary conditions need to be extended to the $m = -1$ and $m = M+1$ spatial points, as the corresponding values y_{-1}^n and y_{M+1}^n are necessary for obtaining y_1^n and

y^n_{M-1} respectively. The new boundary condition is setting the second-order spatial derivative to zero at the boundary, that is

$$\left.\frac{\partial^2 y}{\partial x^2}\right|_{x_0,t_n} = 0 = \left.\frac{\partial^2 y}{\partial x^2}\right|_{x_M,t_n} \quad \forall\, n\,. \tag{3.17}$$

This states that the bending momentum cannot be transferred through the "pinned" boundary [Fletcher 1998]. The numerical stability is proven in [Bensa 2003] as already mentioned. It should be noticed that the magic time-step choice is not valid. The necessary and sufficient stability condition in this case is (for a given sampling rate)

$$X \leq \sqrt{\frac{1}{2}\left(c^2T^2 + 4b_2T + \sqrt{(c^2T^2 + 4b_2T)^2 + 16\kappa^2T^2}\right)}\,.$$

The excitation of the system can be implemented by adding a force density term $\rho^{-1}f(x, x_0, t)$ on the right part of Eq. (3.11), where x_0 denotes the excitation point. The force density has the dimension of force per unit length. This, however, does not affect the discretization much. Equation (3.15) remains as previously, now including an extra force term $a_F F^n_m$, where

$$a_F = \frac{T^2/\rho}{1 + b_1T}\,. \tag{3.18}$$

Further use of the FDM is found in [Giordano 1997], where the soundboard of the piano is modelled, and in [Hikichi 1999], where a complete FDTD piano model is presented.

3.2 Digital waveguides

In 1983 Karplus and Strong introduced the so called *Karplus-Strong algorithm* in [Karplus 1983]. The relationship of the algorithm to the physics of the plucked string was further explored in [Jaffe 1995]. In 1987 the study of the underlying ideas of the algorithm by Smith resulted to the development of the *digital waveguide* theory [Smith 1987] and later to *digital waveguide modelling* (DWM), a method for physics-based sound synthesis [Smith 1992]. While the FDM starts from discretizing the continuous-time wave equation and then solves the resulted discrete-time equation, the DWM directly simulates the general analytical solution in the time-domain. This approach has proven advantageous when employing DSP techniques. Generally speaking, in linear one-dimensional systems such as the string the DWM presents typically stronger computational efficiency than the FDM, whereas this is reversed in multidimensional mesh structures [Välimäki 2006]. A comprehensive introduction to digital waveguide modelling can be found in [Smith 2008]. Especially for the case of two- and three-dimensional systems [Bilbao 2004b] provides an excellent source.

3.2.1 The travelling-wave solution

In 1747 d'Alembert suggested that the general solution to the lossless wave equation (3.1) can be seen as a superposition of two waves travelling in opposite directions along the string [d'Alembert 1747]. The so called *travelling-wave* solution is thus also known as the *d'Alembert solution*.

If

$$\begin{aligned} y^+(x,t) &= f(t-x/c) \\ y^-(x,t) &= h(t+x/c) \end{aligned}$$

denote the right-going and left-going travelling waves respectively, f and h being arbitrary twice-differentiable functions, then the general solution to the wave equation can be expressed as

$$y(x,t) = f(t-x/c) + h(t+x/c)\ . \tag{3.19}$$

Digital waveguide modelling considers directly discretizing the travelling-wave solution. This is possible as long as all initial conditions and excitations are bandlimited to less than half the sampling rate (i.e. the Nyquist frequency) to avoid aliasing [Smith 1992]. Using the same space-time grid as in the finite difference method and choosing always $T = X/c$ yields

$$[y^+]_m^n = f\ (\ t_n - x_m/c\ ) = f\ [\ (n-m)T\ ] = f(n-m)$$

$$[y^-]_m^n = h\ (\ t_n + x_m/c\ ) = h\ [\ (n+m)T\ ] = h(n+m)$$

for the travelling waves. Hence, the string displacement at each grid position is computed by adding the right- and left-going sampled waves

$$y_m^n = f(n-m) + h(n+m)\ . \tag{3.20}$$

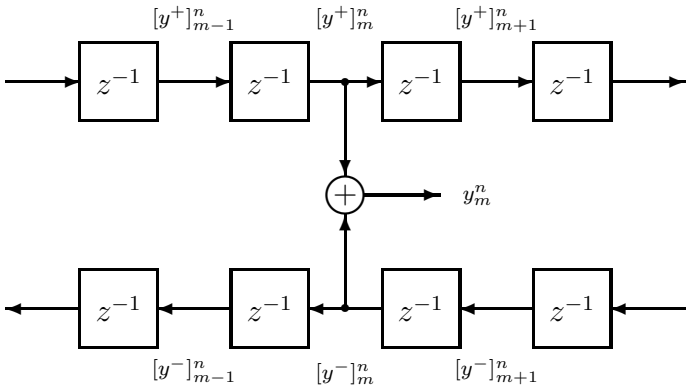

Figure 3.1: The digital waveguide principle.

Accordingly, the value at the next time-step is the sum of the travelling waves shifted by one spatial sample, i.e. $f(n-m+1)$ and $h(n+m+1)$. If each such shift is digitally implemented by a unit delay z^{-1} as illustrated in Fig. 3.1, then the right and left propagation is simply simulated by two delay lines z^{-m}. In the case of infinitely rigid boundary conditions the waves reflect with the same amplitude but opposite sign. This is modelled as shown in Fig. 3.2. In principle, the DWM for the ideal string is exact at the sampling instants.

At this point it is worth examining the relationship of digital waveguide modelling to the finite-difference method. Considering Eq. (3.8), which is the FDTD scheme for the ideal string on the stability bound, and applying decomposition into right- and left-travelling waves on each term results to

$$y_m^{n+1} = f(n-m+1) + h(n+m+1)\,. \tag{3.21}$$

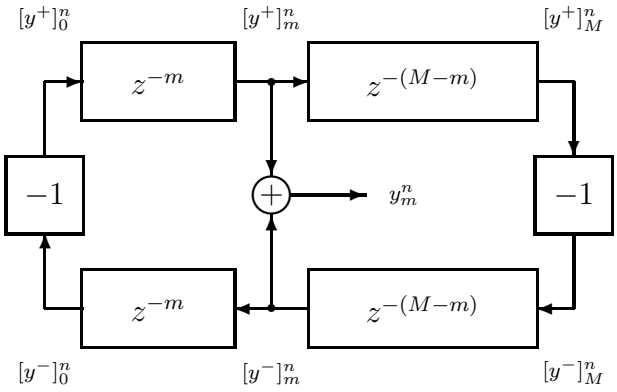

Figure 3.2: Digital waveguide modelling of the ideal string.

Of course, this is the d'Alembert solution. It is thus shown that the DWM is (mathematically) equivalent to the FDM in the case of $\lambda = 1$. Generalizing, digital waveguides are in reality a subclass of FDTD schemes, i.e. on the stability bound. A thorough discussion on this equivalence can be found in [Bilbao 2004b], where the author notes that "[...] there has been almost no attempt to view multidimensional digital waveguide networks as finite difference schemes (which they are). [...] What could these scattering methods be *but* finite difference schemes?"

Excitation of the system When modelling strings it is worth substituting displacement y with velocity v. The reason is that the latter is directly related to force F through the characteristic impedance of the string R as the following formula implies [Morse 1948, Smith 1992]:

$$v = \frac{F}{R}\,, \quad R = \sqrt{T_e \rho}\,. \tag{3.22}$$

Considering the fact that the wave equation (3.1) is linear, the use of alternative wave variables such as velocity, acceleration, slope and force is justified. Accordingly, the excitation of the system—in the form of an external force F_0—can be implemented by introducing an initial velocity v_0 to both delay lines at the excitation point m_0. Since the force is virtually applied on two strings of impedance R, the initial velocity is then given by

$$v_0 = \frac{F_0}{2R} . \tag{3.23}$$

3.2.2 Losses and dispersion

In the case of the stiff and lossy string the effects of air damping, internal friction and string stiffness are modelled with DSP techniques. Considering frequency independent losses the wave equation is written

$$\frac{\partial^2 y}{\partial t^2} = c^2 \frac{\partial^2 y}{\partial x^2} - 2b_1 \frac{\partial y}{\partial t} .$$

It can be shown that the above equation is satisfied by the modified travelling-wave solution

$$y(x,t) = e^{-(b_1/2\rho)x/c} f(t - x/c) + e^{(b_1/2\rho)x/c} h(t + x/c) . \tag{3.24}$$

Sampling as in the ideal string case yields

$$y_m^n = g^{-m} f(n - m) + g^m h(n + m) , \tag{3.25}$$

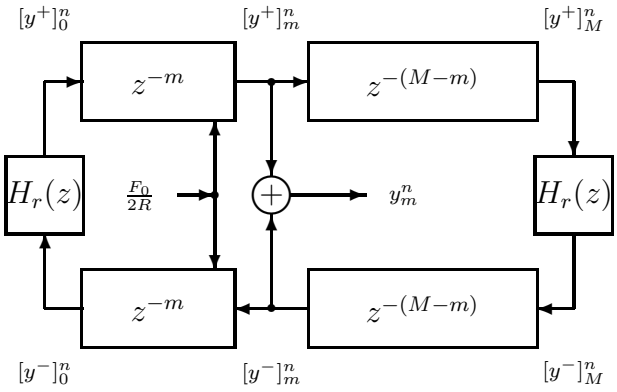

Figure 3.3: Digital waveguide modelling of the non-ideal string.

where $g = e^{-b_1 T/2\rho}$. This can be digitally implemented by attaching gain factors g to each unit delay. Note that although losses are admitted in the wave equation, the solution (3.25) remains exact at each sampling step. To include frequency dependent losses the solution described in (3.24) can be further generalized. Eventually, the factors g in (3.25) are replaced by digital filters $H_g(z)$. These are usually first-order IIR filters, such as the one-pole loss filter suggested in [Välimäki 1996]. Other approaches include second-order FIR filters [Borin 1997].

The stiffness of the string introduces frequency dependent dispersion. The reason is that it causes the waves to propagate faster at high frequencies. This effect can be implemented by allpass filters $H_d(z)$ that have frequency dependent delay, that is larger phase delay at low frequencies. One way to design such filters is using equal first-order allpass filters in series [Van Duyne 1994a]. A more efficient method is proposed in [Rocchesso 1996]. To reduce the computational load for the dispersion filter the study of perceived inharmonicity is considered in [Rocchesso 1999].

It is very important that the phase delay is highly accurate at the fundamental frequency of the note. If not, the note will be out of tune. It is generally better to implement fractional delays by a separate filter $H_f(z)$, rather than including them in the dispersion filter. In [Välimäki 1995] it is proposed to place $H_f(z)$ in series with the delay line. The most common approach is using a first-order allpass filter [Jaffe 1983].

Placing the loss, dispersion and fractional delay filters after each unit delay would automatically raise the computational cost significantly. Now this is a crucial point and the DWM succeeds in overcoming it, thus proving its efficiency. As suggested in [Smith 1992] the effect of all filters can be consolidated at a minimum number of points. This is allowed by the fact that the system is linear and time-invariant. Therefore filters can be placed anywhere in the digital waveguide. Eventually a so called reflection filter $H_r(z) = H_g(z)H_d(z)H_f(z)$ can be used at one side of the digital waveguide as depicted in Fig. 3.3.

Digital waveguide modelling has been a popular method for numerical simulation of the piano. The first piano model based on the DWM was presented in [Garnett 1987]. A different approach based on digital waveguides was introduced in [Van Duyne 1995, Smith 1995], namely the *commuted piano synthesis*. It is regarded as the most efficient digital waveguide piano model [Bank 2000]. A comprehensive overview on digital waveguide modelling of the piano can be found in [Bank 2000]. A research review is provided in [Bank 2003].

3.3 The hammer-string interaction

The sound of the piano is the result of a complex action, as already discussed in Chapter 2. As soon as the hammer strikes the string, an interaction force occurs, which determines the initial excitation of the string. The hammer-string interaction is thus a crucial factor in the resulting sound.

3.3.1 Physical description

As described in Chapter 2, the piano hammer can be considered as a lumped mass connected to a nonlinear spring [Fletcher 1998, Bank 2003]. This is expressed at the excitation point x_0 by the equation

$$M_H \frac{d^2\eta}{dt^2} = -F_H \ , \tag{3.26}$$

where $\eta(t)$ is the hammer displacement, M_H is the hammer mass, and $F_H(t)$ is the occurring interaction force or hammer force, i.e. the force due to the hammer felt. Experimental measurements of real pianos suggest that the hammer force is a nonlinear function of the compression of the hammer felt $\xi(t)$ [Hall 1992, Chaigne 1994a, Fletcher 1998]. The nonlinearity is described by the power law (2.1):

$$F_H(t) = \phi[\xi(t)] = K\,\xi(t)^{\,p} \ , \ \ \xi(t) = \,|\,\eta(t) - y(x_0,t)\,|\,. \tag{3.27}$$

Real piano hammers, however, exhibit hysteretic behaviour, as suggested in [Fletcher 1998]. That is, the hammer-string interaction force is rather defined by the history of the compression. Therefore, the above equation is

not fully satisfactory. A model with hysteresis was proposed in [Stulov 1995]. According to the mechanics of solids [Bank 2003], a time-dependent operator needs to be inserted in (3.27), to introduce hysteresis. This time-dependent operator is essentially a so called *relaxation function* that accounts for the "memory" of the material [Stulov 1995, Bank 2003]. The modified equation for the hammer force is then

$$F_H(t) = \phi[\xi(t)] = K[1 - r(t)] * \xi(t)^{\,p} \tag{3.28a}$$

$$r(t) = (\sigma/\tau)e^{-t/\tau} \ , \tag{3.28b}$$

where $r(t)$ is the relaxation function, σ and τ are hysteresis and relaxation constants respectively, and the $*$ operator denotes convolution.

3.3.2 Modelling approaches

Considering the above equations, the hammer-string interaction can be modelled by discretizing the differential equation (3.26), and by directly putting Eqs. (3.27) or (3.28) in discrete form. Such an approach was proposed in [Chaigne 1994a, Chaigne 1994b] using an FDTD scheme. Furthemore, a similar power law model was applied to the DGM in [Borin 1992]. Direct implementation of the hammer-string interaction model can be advantageous, as it allows the spectrum of the output signal to vary dynamically with the initial velocity—a characteristic feature of the real piano sound [Bank 2000]. Moreover, it is a simple and straightforward approach. However, stability

issues arise for high frequency notes when the stiffness and initial velocity values increase [Borin 1996, Borin 1997]. The reason is the implicit nature of the power law. A closer inspection shows that the hammer position at the present time-step η^n should be known for obtaining the contact force at the same instant $F_H(n)$, and vice versa. This implicit formula can be made explicit by assuming that $F_H(n) \approx F_H(n-1)$, that is by inserting a fictitious delay element in a delay-free path [Borin 1997, Bank 2003]. As a result of this approximation, the system tends to become unstable in the high register of the piano. To overcome this, a different approach is suggested in [Borin 1996, Borin 1997], which is based on solving analytically the implicit equation for integer values of the stiffness exponent. This model also takes hysteresis into account by discretizing the equations in [Stulov 1995]. However, computing the interaction force in such a way can be very complicated. Also, analytical solution of the implicit equation for fractional stiffness exponents is not possible due to the large number of computations demanded. In [Borin 1996] it is also suggested that implementing the relaxation function as a first-order low-pass filter can produce results that are in good agreement with real data.

A first FDTD approach to modelling the hammer-string interaction can be found in the early numerical simulations of Hiller and Ruiz [Hiller 1971a, Hiller 1971b]. However, according to Chaigne and Askenfelt, the work of Bacon and Bowsher [Bacon 1978] can be considered as the first serious time-domain simulation of the hammer-string interaction. In the first case, the hammer-string contact duration was set beforehand as a known parameter—in reality it is a result of the hammer-string interaction. In the latter,

there were several miscalculations, e.g. the stiffness of the string was omitted. Other approaches using the FDM include the works of [Boutillon 1988], [Suzuki 1987], [Hall 1992], and [Chaigne 1994a, Chaigne 1994b].

Another method to model the hammer-string interaction is by considering wave digital filters and is known as the *wave digital filter*, first proposed in [Van Duyne 1994b, Van Duyne 1994c]. The string is modelled using the DWM, and the distributed hammer model is attached to the digital waveguide by a scattering junction. The spring is considered linear; the nonlinear characteristic of the felt is implemented by the stiffness coefficient by reading compression-correspondent values from a lookup-table. Hysteresis can also be taken into account by readjusting the pointer in the table, according to the velocity of the felt compression [Bank 2000]. The drawback of this approach is its complexity.

Commuted piano synthesis provides a different approach for the hammer model [Smith 1995, Van Duyne 1995]. The hammer is implemented by a linear filter. The novelty of this method lies in that the parameters of the linear filter are obtained by nonlinear simulation. However, this implies that the hammer filter must be designed for all strings and dynamic levels. A nonlinear model is generally preferred, as it responds to the initial velocity in a more physically meaningful way [Bank 2000]. Another disadvantage of this method is its inability to account for the re-striking of the string by the hammer [Bank 2000].

A thorough discussion on issues regarding the modelling of the hammer-string interaction can be found in [Bank 2000], where a new technique is also presented, the so called *multi-rate hammer*. The basic idea of this method

is running the hammer model at a double sampling rate than that of the string model. Simulation results suggest better stability than operating both the string and hammer models at the same sampling rate. Hysteresis can be easily implemented as well. Most recently, a source-resonator model of hammer-string interaction was proposed in [Bensa 2004].

3.4 Discussion

Modelling the string is a core element of modelling stringed instruments, thus a crucial step in the process of modelling the piano. Finite differences and digital waveguides provide two different—but equivalent as already discussed—approaches, the first using applied mathematics, and the latter digital signal processing techniques. The FDM is more physically meaningful, but it can become quite complicated and computationally expensive. The DWM, on the other hand, is computationally cheap, but lacks much of the physicality inherited in the FDM. Digital waveguide modelling remains the most efficient method for modelling the one-dimensional string, and thus the most popular. A different approach is provided by modal synthesis.

Modal synthesis was introduced in [Adrien 1991]. It describes the system in terms of its modes of vibration. A vibrating mode is a particular motion such that every point of the mechanism vibrates at the same frequency. The approach is summarized in that any vibration of the mechanism can be expressed as the sum of the contributions of its modes. Although in theory there are infinite modes of vibration corresponding to infinite degrees of freedom, practically for simple structures, such as strings, spatial discretization is required for analytical determination of modal data. This leads to reduction

of the degrees of freedom, hence of the number of possible modes, to a finite number. This constitutes a limitation, which can be overcome with the functional transformation method (FTM) [Trautmann 2003]. The FTM forms a novel approach to modal synthesis. Starting with directly solving the PDEs of the physical model analytically, it applies two different integral transformations to remove the partial derivatives, i.e. a Laplace transform (time) and a Sturm-Liouville transform (space). As a result, spatial discretization is avoided, as accurate models of vibrating strings and membranes can be built without the need for data determination [Välimäki 2006]. Accordingly, the FTM seems to be both an efficient and accurate numerical simulation method for strings. It retains the physics of the system like the FDM, while being less computationally expensive.

Further on piano physical modelling, a different approach considering longitudinal displacement of piano strings is presented in [Bank 2004], where a finite-difference scheme modelling transversal vibrations is used to drive second-order resonators for longitudinal vibration simulation.

Chapter 4

Model design and simulation

The piano model described below is designed within the context of the present investigation. Accordingly, it considers a stiff and lossy string with scalar impedance on both ends, excited by a hammer, and implementing the hammer string-interaction. Modelling other parts and properties of the instrument is omitted, as it is of no interest to the purposes of the actual investigation. Similarly, hysteresis of the hammer felt is not taken into account. Section 4.1 follows the building of the model, while Sections 4.2 and 4.3 consider finite-difference time-domain and digital waveguide simulation respectively. Finally, Section 4.4 provides the model parameters.

4.1 Model structure

The analytical wave equation for the stiff and lossy string is (see 3.1.3)

$$\frac{\partial^2 y}{\partial t^2} = c^2 \frac{\partial^2 y}{\partial x^2} - \kappa^2 \frac{\partial^4 y}{\partial x^4} - 2b_1 \frac{\partial y}{\partial t} + 2b_2 \frac{\partial^3 y}{\partial x^2 \partial t} + \rho^{-1} f(x, x_0, t) \; . \qquad (4.1)$$

The force density term f represents the excitation of the string by the hammer according to the following relationship [Chaigne 1994a]:

$$f(x, x_0, t) = f_H(t)\, g(x, x_0)\ , \tag{4.2}$$

where x_0 is the excitation position, $g(x, x_0)$ is a dimensionless spatial window that corresponds to the hammer width, and $f_H(t)$ refers to the time history of the hammer force $F_H(t)$ on the string as indicated by the expression below [Chaigne 1994a]:

$$f_H(t) = F_H(t) \left(\int_{x_0-\delta x}^{x_0+\delta x} g(x, x_0) dx \right)^{-1} \ . \tag{4.3}$$

The part of the string that interacts with the hammer has a length of $2\,\delta x$. The displacement $\eta(t)$ of the hammer felt is defined by the equation

$$M_H \frac{d^2\eta}{dt^2} = -F_H(t) - b_H \frac{d\eta}{dt}\ , \tag{4.4}$$

which takes into account air damping. Finally, the force $F_H(t)$ exerted by the hammer on the string is given by the power law already discussed in Section 2.3 and Section 3.3:

$$F_H(t) = K\, |\, \eta(t) - y(x_0, t)\, |^{\,p}\ . \tag{4.5}$$

Boundary conditions at the bridge are given by

$$F_b = R_b \frac{\partial y}{\partial t}\ , \tag{4.6a}$$

and

$$\left.\frac{\partial^2 y}{\partial x^2}\right|_{x_M,t_n} = 0 \,, \tag{4.6b}$$

where R_b is the impedance of the bridge, and F_b is the force imposed by the string on the bridge. If the damping terms are locally ignored, then the latter can be expressed as

$$F_b = -T_e \frac{\partial y}{\partial x} + \kappa^2 \rho \frac{\partial^3 y}{\partial x^3} \,. \tag{4.6c}$$

By combining Eqs. (4.6a) and (4.6c) the first boundary condition may be written as

$$-T_e \frac{\partial y}{\partial x} + \kappa^2 \rho \frac{\partial^3 y}{\partial x^3} = R_b \frac{\partial y}{\partial t} \,. \tag{4.6d}$$

or

$$\frac{\partial^3 y}{\partial x^3} = \frac{c^2}{\kappa^2}\frac{\partial y}{\partial x} + \frac{\zeta_b c}{\kappa^2}\frac{\partial y}{\partial t} \,, \tag{4.6e}$$

where $\zeta_b = R_b/\rho c$ is the normalized bridge impedance. Boundary conditions at the left hinged end are similarly given by

$$\frac{\partial^3 y}{\partial x^3} = -\frac{c^2}{\kappa^2}\frac{\partial y}{\partial x} + \frac{\zeta_l c}{\kappa^2}\frac{\partial y}{\partial t} \,, \tag{4.7a}$$

and

$$\left.\frac{\partial^2 y}{\partial x^2}\right|_{x_0,t_n} = 0 \,, \tag{4.7b}$$

where $\zeta_l = R_l/\rho c$ is the normalized impedance of the left end.

Summarizing, the string-hammer model consists of the partial differential equations (4.1) and (4.4), and the right and left boundary conditions (4.6) and (4.7) respectively.

4.2 Finite-difference modelling

In the previous Chapter the approximation of the wave equation for the stiff and lossy string with the finite-difference time-domain method has been discussed (see Section 3.1). Accordingly, the discrete-time expression for Eq. (4.1) is

$$\begin{aligned} y_m^{n+1} &= a_1(y_{m+2}^n + y_{m-2}^n) + a_2(y_{m+1}^n + y_{m-1}^n) + a_3 y_m^n \\ &\quad + a_4 y_m^{n-1} + a_5(y_{m+1}^{n-1} + y_{m-1}^{n-1}) + a_F F_m^n \ , \end{aligned} \tag{4.8}$$

where the coefficients a_i and a_F are the ones defined in (3.16) and (3.18), and the discrete-time force density term is defined as [Chaigne 1994a]

$$F_m^n = F_H(n)\, g(m, m_0) \ . \tag{4.9}$$

However, Eq. (4.8) is valid only in the "interior" of the string, i.e. for $m = 2, 3, \ldots, M-2$. To compute the corresponding formula for the points just off the boundary, as well as at the boundary, the related conditions are needed. Condition (4.6b) is numerically expressed as

$$y_{M+1}^n = 2y_M^n - y_{M-1}^n \ . \tag{4.10}$$

For $m = M - 1$ the previous becomes

$$y_{m+2}^n = 2y_{m+1}^n - y_m^n \, . \tag{4.11}$$

Substituting into Eq. (4.8) gives the updated formula for the point just off the bridge:

$$\begin{aligned} y_m^{n+1} &= a_1(2y_{m+1}^n - y_m^n + y_{m-2}^n) + a_2(y_{m+1}^n + y_{m-1}^n) + a_3 y_m^n \\ &\quad + a_4 y_m^{n-1} + a_5(y_{m+1}^{n-1} + y_{m-1}^{n-1}) + a_F F_m^n \ . \end{aligned} \tag{4.12}$$

Considering condition (4.7b) at the left boundary, expression (4.11) is re-written as

$$y_{m-2}^n = 2y_{m-1}^n - y_m^n \, , \tag{4.13}$$

thus the updated formula for $m = 1$ is

$$\begin{aligned} y_m^{n+1} &= a_1(y_{m+2}^n - y_m^n + 2y_{m-1}^n) + a_2(y_{m+1}^n + y_{m-1}^n) + a_3 y_m^n \\ &\quad + a_4 y_m^{n-1} + a_5(y_{m+1}^{n-1} + y_{m-1}^{n-1}) + a_F F_m^n \ . \end{aligned} \tag{4.14}$$

Obtaining the relevant expressions for the points at the bridge and at the left boundary is not as trivial. Rather the finite-difference approximations of the conditions (4.6e) and (4.7a) are applied. The hence necessary centered

operator for the third-order partial space derivative of y is defined as

$$\left.\frac{\partial^3 y}{\partial x^3}\right|_{m,n} = \frac{y^n_{m+2} - 2y^n_{m+1} + 2y^n_{m-1} - y^n_{m-2}}{2X^3} \,. \tag{4.15}$$

Substituting into Eq. (4.6e) gives

$$\begin{aligned} y^n_{m+2} &= [2+\mu^{-1}](y^n_{m+1} - y^n_{m-1}) \\ &+ [\zeta_b \lambda^{-1}\mu^{-1}](y^{n+1}_m - y^{n-1}_m) \\ &+ y^n_{m-2} \,. \end{aligned} \tag{4.16}$$

Substitution into Eq. (4.8) results in

$$\begin{aligned} [1 - a_1\zeta_b\lambda^{-1}\mu^{-1}]y^{n+1}_m &= [a_2 + a_1(2+\mu^{-1})]y^n_{m+1} \\ &+ a_3 y^n_m \\ &+ [a_2 - a_1(2+\mu^{-1})]y^n_{m-1} \\ &+ 2a_1 y^n_{m-2} \\ &+ [a_4 - a_1\zeta_b\lambda^{-1}\mu^{-1}]y^{n-1}_m \\ &+ a_5(y^{n-1}_{m+1} + y^{n-1}_{m-1}) \\ &+ a_F F^n_m \,. \end{aligned} \tag{4.17}$$

Finally, considering

$$y^n_{m+1} = 2y^n_m - y^n_{m-1}$$

$$y^{n-1}_{m+1} = 2y^{n-1}_m - y^{n-1}_{m-1} \,,$$

and substituting into (4.17) yields

$$y^{n+1}_m = b_{R1}y^n_m + b_{R2}y^n_{m-1} + b_{R3}y^n_{m-2} + b_{R4}y^{n-1}_m + b_{RF}F^n_m \,, \tag{4.18}$$

where b_{Ri} and b_{RF} are the convenient coefficients

$$b_{R1} = \frac{2 - 2\lambda^2\mu - 2\lambda^2}{1 + b_1 T + \zeta_b \lambda} \tag{4.19a}$$

$$b_{R2} = \frac{4\lambda^2\mu + 2\lambda^2}{1 + b_1 T + \zeta_b \lambda} \tag{4.19b}$$

$$b_{R3} = \frac{-2\lambda^2\mu}{1 + b_1 T + \zeta_b \lambda} \tag{4.19c}$$

$$b_{R4} = \frac{-1 + b_1 T + \zeta_b \lambda}{1 + b_1 T + \zeta_b \lambda} \tag{4.19d}$$

$$b_{RF} = \frac{T^2/\rho}{1 + b_1 T + \zeta_b \lambda} \ . \tag{4.19e}$$

Equation (4.18) provides the numerical expression at the bridge boundary $m = M$. After repeating the same discretization process for Eq. (4.7a) the corresponding expression at the left boundary $m = 0$ is obtained:

$$y_m^{n+1} = b_{L1} y_m^n + b_{L2} y_{m+1}^n + b_{L3} y_{m+2}^n + b_{L4} y_m^{n-1} + b_{LF} F_m^n \ . \tag{4.20}$$

The coefficients b_{Li} and b_{LF} are equal to the b_{Ri} and b_{RF} respectively, but in this case the normalized impedance ζ_l of the left boundary is used instead of the bridge normalized impedance ζ_b .

To discretize the hammer displacement differential equation (4.4) the following centered operators are used:

$$\left.\frac{d^2\eta}{dt^2}\right|_n = \frac{\eta^{n+1} - 2\eta^n + \eta^{n-1}}{T^2}$$

$$\left.\frac{d\eta}{dt}\right|_n = \frac{\eta^{n+1} - \eta^{n-1}}{2T} \ .$$

Substituting in (4.4) yields the numerical expression

$$\eta^{n+1} = d_1\eta^n + d_2\eta^{n-1} + d_F F_H(n) \ , \tag{4.21}$$

where

$$d_1 = \frac{2}{1 + b_H T/2M_H} \tag{4.22a}$$

$$d_2 = \frac{-1 + b_H T/2M_H}{1 + b_H T/2M_H} \tag{4.22b}$$

$$d_F = \frac{-T^2/M_H}{1 + b_H T/2M_H} \ , \tag{4.22c}$$

are convenient coefficients. To complete the main "loop" of the simulation algorithm, the value of the hammer force at the present step is demanded to calculate the value of the hammer displacement at the next time-step. This is obtained by the numerical correspondent of the power law (4.5):

$$F_H(n) = K \, | \, \eta^n - y^n_{m_0} \, |^{\, p} \ . \tag{4.23}$$

4.3 Digital waveguide modelling

The aim of the present investigation is to build and compare two equivalent hammer-string models, the one with finite differences and the other with digital waveguides. However, there seems to be no obvious way of modelling a spatially distributed hammer force excitation with the DWM, as discussed in 3.3.2. Furthermore, the filter design would cause the digital waveguide model to have effective differences from the FDTD model. This would be undesired, because the two models need to have as less differences as possible, to allow the aimed experiments. To overcome such complications, a digital waveguide model is avoided altogether, and a hybrid structure based on the FDTD model is used instead.

The main idea of this approach is keeping the FDTD model for the string and hammer displacement, but setting the string stiffness to zero, so as to fit the general DWM theory, according to which the two stiffness-related solutions of the wave equation are omitted. To model fractional delays and losses, specific filters are supplied to the boundaries of the FDTD model. These filters are designed so as to function in the exact same way as the allpass filters in the DWM (see 3.2.2). To interconnect the FDTD model with the boundary filters, the use of KW-converters is necessary.

Physical variables, such as the string displacement y_m^n , are often referred to as *K-variables*, with a reference to their Kirchhoff type. Similarly, FDTD models are called *K-models*. In the case of travelling wave decomposition, the variables are referred to as *W-variables*, and the corresponding models as *W-models* [Karjalainen 2004]. A KW-converter makes it possible to interconnect a K-model to a W-model and vice versa.

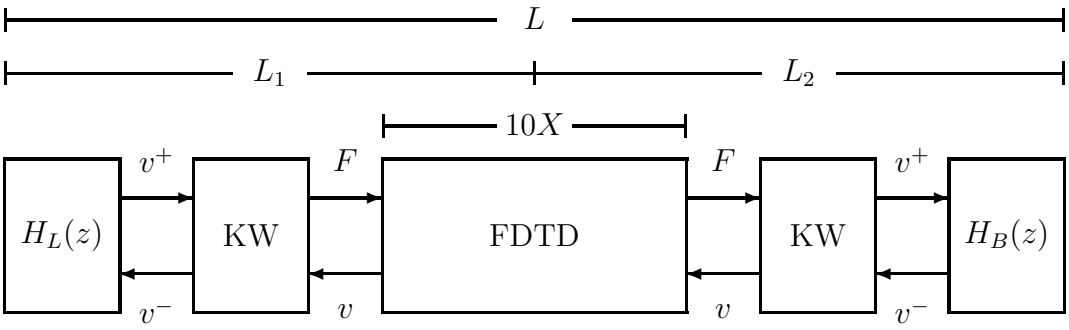

Figure 4.1: The mixed model. The string stiffness in the FDTD model is zero. The KW-converters supply the boundary filters to the FDTD model by changing the force K-variable to the velocity W-variable.

The resulting mixed model is depicted in Fig. 4.1. The boundary allpass filters are designed according to [Rocchesso 1996]. The frequency response of each filter is given by

$$H_B(k,\omega) = r_B\, e^{-2jk(\omega)(L_2-5X)} \tag{4.24a}$$

$$H_L(k,\omega) = r_L\, e^{-2jk(\omega)(L_1-5X)}\ , \tag{4.24b}$$

where $r_B = (1-\zeta_b)/(1+\zeta_b)$ is the reflectance of the bridge, and $r_L = -1$ is the reflectance of the left boundary. The wavenumber k is expressed as a function of the angular frequency $\omega = 2\pi f$ [Bensa 2003]:

$$k(\omega) \simeq \pm\,\frac{c}{\kappa\sqrt{2}}\sqrt{-1+\sqrt{1+4\kappa^2\omega^2/c^4}}\ .$$

To obtain the impulse response of the system, an inverse fast Fourier transformation is applied to the frequency response. Furthermore, in order to

Table 4.1: Values of the model parameters.

	C2	**C4**	**C7**	
String				
f_1	52.8221	262.1895	2112.1	Hz
L	1.92	0.62	0.09	m
M_S	35×10^{-3}	3.93×10^{-3}	0.467×10^{-3}	Kg
T_e	750	670	750	N
b_1	0.25	1.1	9.17	s^{-1}
b_2	7.5×10^{-5}	2.7×10^{-4}	2.1×10^{-3}	s
ϵ	7.5×10^{-6}	3.82×10^{-5}	8.67×10^{-4}	
Hammer				
M_H	4.9×10^{-3}	2.97×10^{-3}	2.2×10^{-3}	Kg
p	2.3	2.5	3.0	
b_H	1×10^{-4}	1×10^{-4}	1×10^{-4}	s^{-1}
K	4×10^{8}	4.5×10^{9}	1×10^{12}	
a	0.12	0.12	0.0625	
Boundary				
ζ_l	1×10^{20}	1×10^{20}	1×10^{20}	$\Omega/Kg.m^{-2}.s^{-1}$
ζ_b	1000	1000	1000	$\Omega/Kg.m^{-2}.s^{-1}$
Sampling				
f_s	4×44.1	4×44.1	4×44.1	kHz
M	521	140	23	

allow a higher order and accurate filter design, delays from the "string" had to be "stolen." As a consequence, the numerical experiments with boundaries are restricted to strings C2 and C4 (see 5.2), as there is not enough length available to extract the required amount of delays for the short C7 string.

Building a mixed model in the place of a pure digital waveguide model has been beneficial. The excitation and the losses are simulated in the exact same way as with the FDTD scheme, providing a uniform platform for the experiments. Most importantly, the mixed model inherits precisely the desired feature of accepting only two of the four solutions of the wave equation.

4.4 Model parameters

The values of the parameters are taken from the simulations of Chaigne and Askenfelt [Chaigne 1994b]. However, appropriate alterations have been made in several cases to better fit the purposes of the present investigation. Table 4.1 gathers the values considered in the numerical experiments.

Chapter 5

Numerical experiments

To investigate the effect of string stiffness on the hammer-string interaction in the context of piano synthesis, numerical experiments were realized by simulating the two models described in the previous Chapter using MATLAB. The results of the experiments include the study of the (hammer) contact force signal over time for different initial velocity values. Synthesized sounds-notes were also recorded and considered. A detailed presentation and discussion of the obtained results follows.

5.1 Case I: Making the string anechoic

Choosing a unit normalized impedance at both ends of the string implies that the impedance of the string is the same to that of the rigid boundary. Such an approach allows a first insight into the effect of neglecting the stiffness of the string in the DWM.

Once the string is made anechoic, that is there are no right and left boundaries, the digital waveguide model becomes exactly the FDTD model with zero damping coefficients. Therefore, it is avoided and the latter is used instead, first with the stiffness and damping parameters set to the values

found in Table 4.1, and then with the same parameters set to zero.

Following the experiments of Chaigne and Askenfelt [Chaigne 1994b], the model simulates the piano strings C2, C4, and C7. Studying each string separately, the initial velocity is set at the three different values of 1 m/s, 2.5 m/s, and 5 m/s. Figures 5.1(a), 5.1(b), and 5.2(a) show the C4, C7, and C2 strings respectively. A first observation is that the influence of the string stiffness increases with initial velocity. However, this does not apply in the case of the C7 string, as the two models behave in an almost exact way. Generally, considering the stiffness of the string does not seem to have an noticeable effect when the string is made anechoic.

A further experiment was attempted, where the stiffness parameter value for the C2 string was increased by a factor of four. The objective was to examine a case of exaggeration. Figure 5.2(b) clearly indicates that then the impact of the string stiffness becomes significantly stronger.

5.2 Case II: Scalar impedance at both ends

The normalized impedance at the right and left boundary is set to the values found in Table 4.1. As mentioned earlier (see 4.3), the numerical experiments in this case are restricted to strings C2 and C4. However, including boundaries allows recording the sounding output of the models.

5.2.1 Graphs

Figures 5.3(a) and 5.4 depict the C2 and C4 strings respectively. It becomes immediately apparent, that in the more real case of considering scalar impedance at both ends, string stiffness is a crucial parameter in the hammer-string interaction. Its effect grows considerably as initial velocity increases.

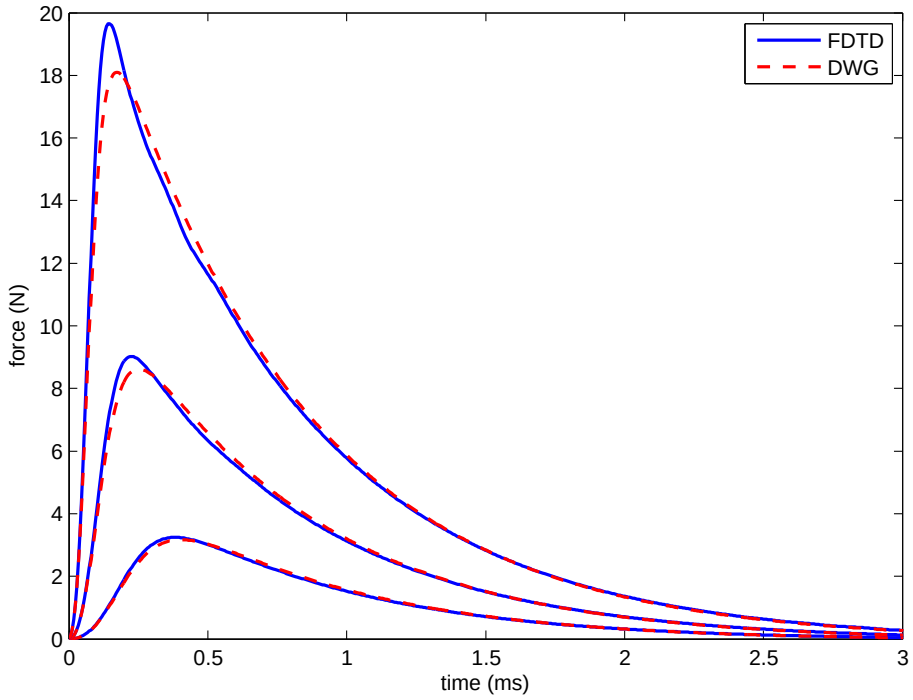

(a) C4

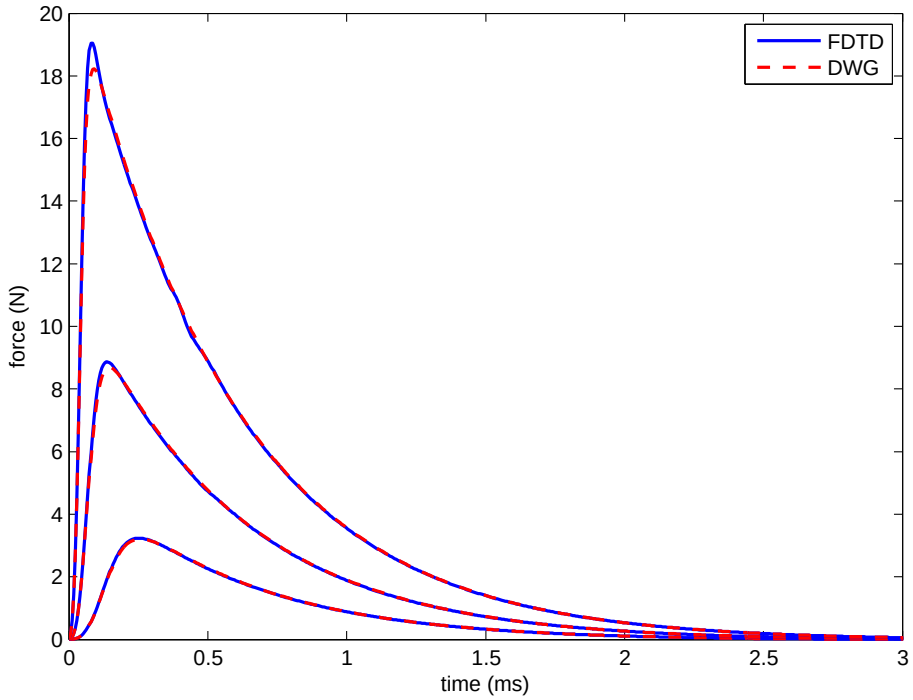

(b) C7

Figure 5.1: Contact force signal for the anechoic C4 and C7 strings with initial velocity set at 1 m/s, 2.5 m/s, and 5 m/s bottom to top respectively.

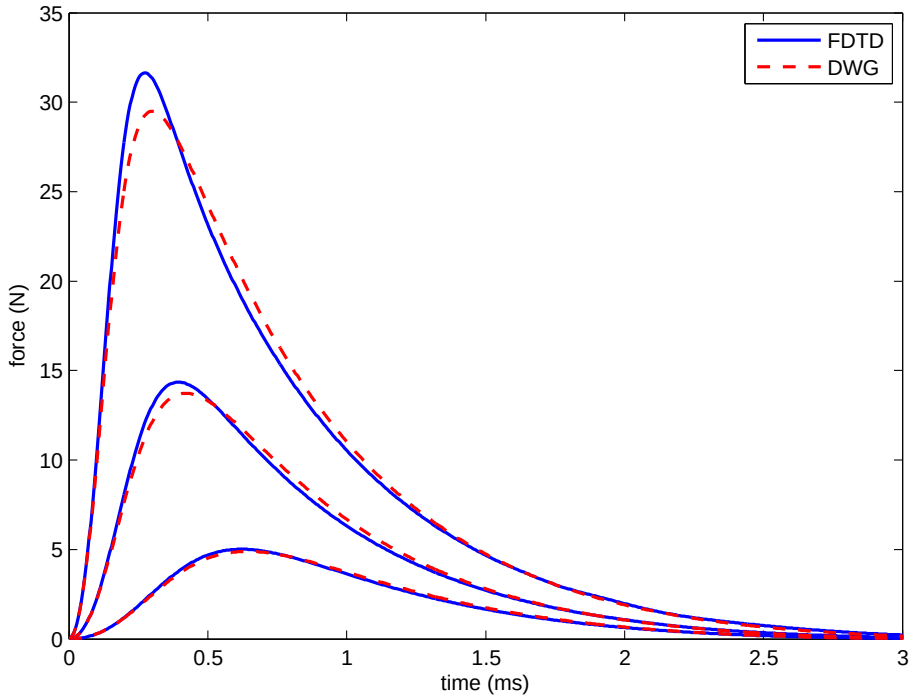

(a)

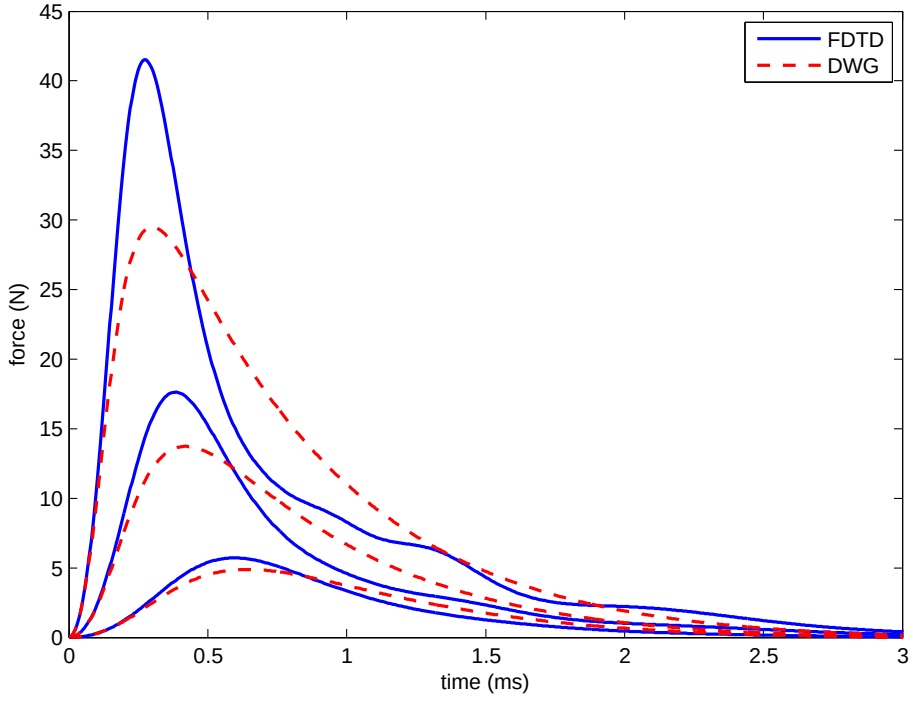

(b)

Figure 5.2: (a) Contact force signal for the anechoic C2 string with initial velocity set at 1 m/s, 2.5 m/s, and 5 m/s bottom to top respectively. (b) Increasing the stiffness parameter value by a factor of four.

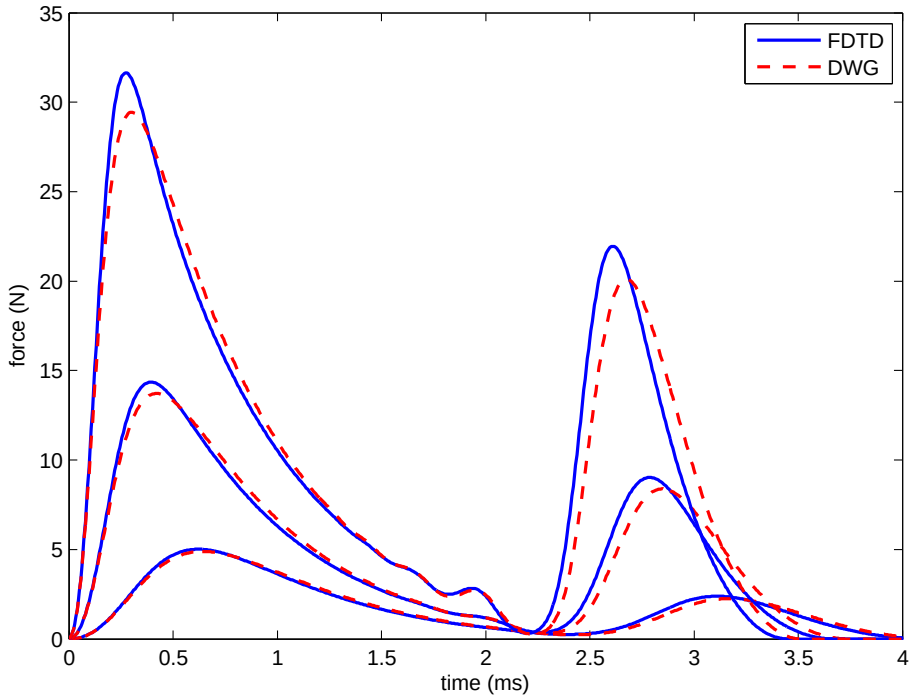

(a)

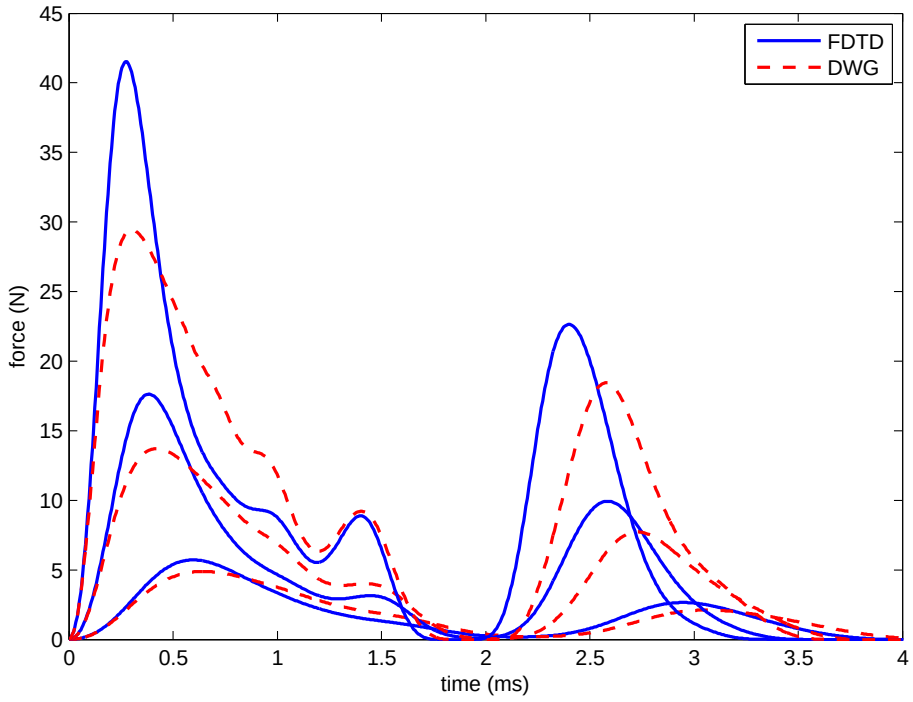

(b)

Figure 5.3: (a) Contact force signal for the C2 string with scalar impedance at both ends, and initial velocity set at 1 m/s, 2.5 m/s, and 5 m/s bottom to top respectively. (b) Increasing the stiffness parameter value by a factor of four.

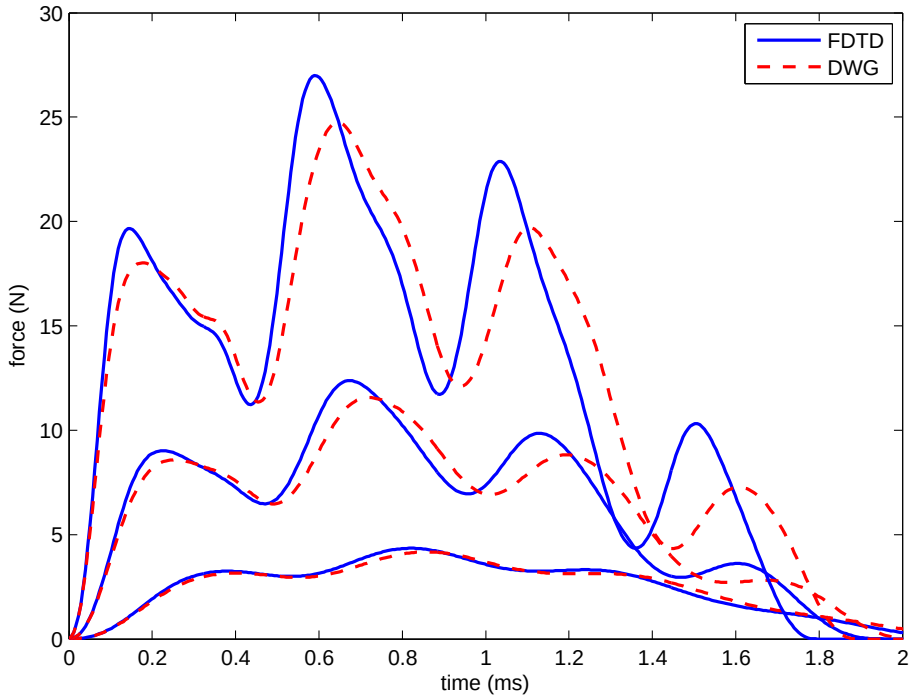

Figure 5.4: Contact force signal for the C4 string with scalar impedance at both ends, and initial velocity set at 1 m/s, 2.5 m/s, and 5 m/s bottom to top respectively.

Furthermore, results seem to be in relatively good agreement with previous experiments [Chaigne 1994b, Bank 2000]. Repeating a similar case of exaggeration for the C2 rigid string, confirmed that the digital waveguide model behaves rather differently from the FDTD model when the stiffness parameter is increased, as shown in Fig. 5.3(b).

5.2.2 Sounds

As underlined in the Introduction, the purpose of this dissertation is to investigate the results of Ducasse in the context of synthesized sound. Listening to the sounding output of each modelling case (FDTD, DWM, initial

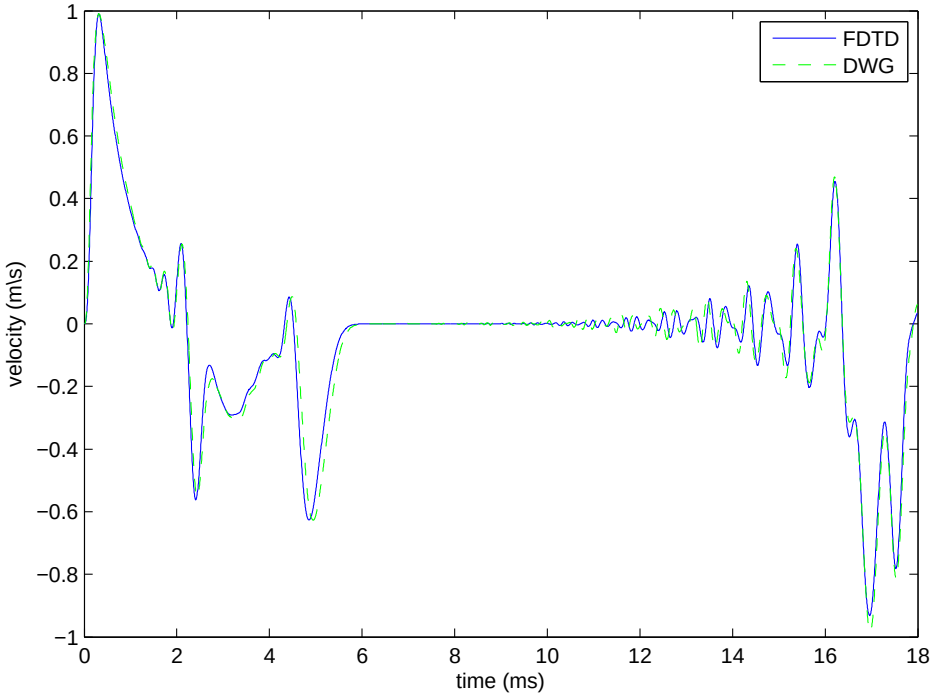

(a)

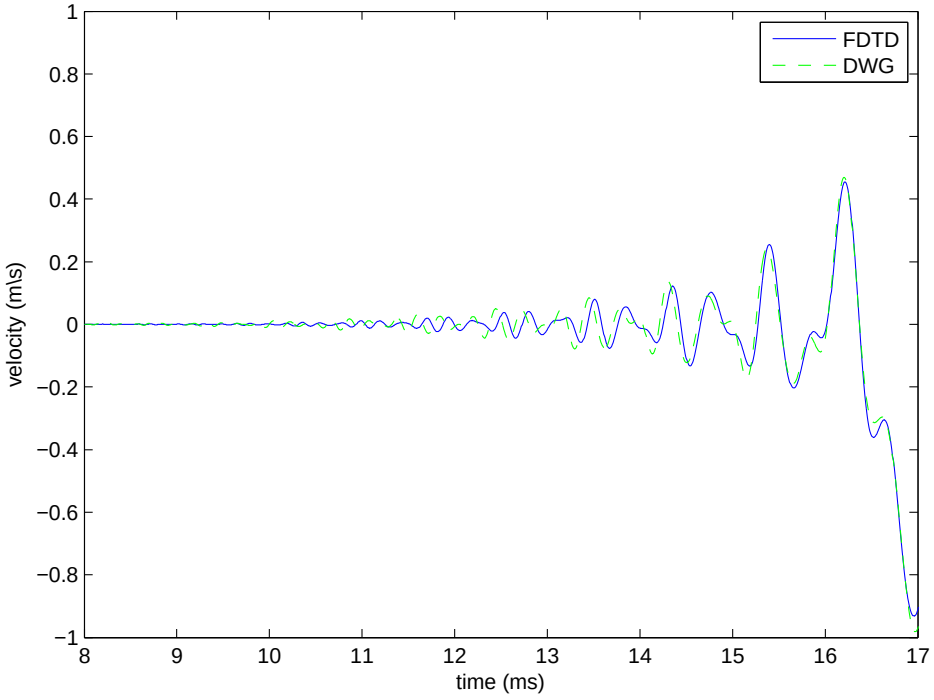

(b)

Figure 5.5: (a) Contact point string velocity for the C2 string with scalar impedance at both ends, and initial velocity set at 5 m/s. (b) Detail of the first precursor.

velocity, increased string stiffness), provided a perceptual approach to the experiments.

Overall, the resulted sounds do not appear to have any distinguished audible differences. However, there is an interesting exception. This corresponds to the more natural case of the C2 string struck with an initial velocity of 5 m/s. A close inspection shows that the first precursor in the digital waveguide model builds in a different way than in the FDTD model, resulting in a more artificially sounding output. Figure 5.5 illustrates the first 18 ms of the string velocity at the contact point, zooming in the building of the first precursor.

This last result exemplifies a more general finding: The string stiffness is an important factor to consider (in the hammer-string interaction) for the bass register of the piano. Its effect becomes less noticable while moving to the mid-frequency region and beyond.

Chapter 6

Conclusions

> Last night I dreamt I went to Manderlay again.
> –Daphne de Maurier, *Rebecca.*

This dissertation presented a physical model for the piano string with scalar impedance at both ends. The hammer-string interaction was studied and implemented. The numerical simulation of the model was realized using both a finite-difference time-domain scheme and a digital waveguide model. The aim was to investigate the effect of string stiffness on the hammer-string interaction. This was motivated by the fact that in the case of digital waveguide modelling the two fast-decaying, stiffness-related travelling waves, which form two of the four solutions to the wave equation of the stiff and lossy string, are omitted [Bensa 2003]. A recent theoretical study [Ducasse 2005] argues that no solutions can be neglected, at least not around the striking point, and suggests that the digital waveguide model presented in [Bensa 2003] needs to be corrected accordingly. The objective of this dissertation was to further investigate this correction in the context of sound synthesis.

Starting from a basic introduction to the acoustics of the piano in Chapter 2, the investigation focused on the hammer-string interaction. Its physics, as well as the various modelling approaches were studied and discussed in

Chapter 3. The design and discrete-time simulation of the model used for the numerical experiments were presented in Chapter 4. Finally, the results were presented and discussed in Chapter 5.

The results overall indicated that the stiffness of the string affects the hammer-string interaction significantly while increasing the initial velocity, most noticeably in the low register of the instrument. This shows generally good agreement with previous experiments. When increasing the stiffness by an exaggerating factor of four, the impact of the string stiffness becomes much stronger, especially for high initial velocity values. In terms of the synthesized sounds, listening to the them showed no perceivable differences, except for the C2 string with an initial velocity of 5 m/s. In this case the DWM output sounds more artificial. Finally, when considering unit impedance at both ends, string stiffness seems to be less effective.

The present investigation hopes to have contributed towards efficient physics-based sound synthesis of the piano. Future experiments may consider a complete piano model, that is implementing the soundboard, and/or the beating and two-stage decay of coupled strings, and further investigate the effect of string stiffness on the hammer-string interaction in this context. Furthermore, formal listening tests might be necessary to better determine whether or not the quality of the synthesized sounds would be considerably improved.

Acknowledgments

I started writing this dissertation in Belfast and completed it in Montréal.

I am deeply indebted to my parents. It is to their love and trust, and to their generous support that I owe my educational adventures.

I would like to thank my friends in Greece for being always there for me—especially Anastasia for the endless skype talks!

I would like to thank my supervisor Maarten van Walstijn for his guidance and ... patience! I consider myself lucky to have been his student. I am grateful to him for having drawn my attention to the area of physical modelling, as well as encouraging my next steps.

Many thanks to all the people at the **S**onic **A**rts **R**esearch **C**entre for making this an exciting year. Special thanks to Sile O'Modhrain who convinced me into joining the MA course, and Pearl for making things easier.

Special thanks to wasilakis (aka Vasileios Chatziioannou) for sharing his knowledge, and for joining me for beers at The Spaniard and cappuccinos at Clements!

Finally, I am grateful to my classmates (aka fellow-students), who made life at the University so much easier!

Bibliography

[Adrien 1991] Adrien, J.-M. "The missing link: Modal synthesis." In G. De Poli, A. Piccialli, and C. Roads (eds.) *Representations of Musical Signals*. Cambridge, MA: The MIT Press. 1991, pp. 269–297.

[Bacon 1978] Bacon, R. A. and Bowsher, J. M. "A discrete model of a struck string," *Acustica*, vol. **41**, 1978, pp. 21–27.

[Bank 2000] Bank, B. (2000). *Physics-based Sound Synthesis of the Piano*. Master thesis, Budapest University of Technology and Economics, Budapest, Hungary. Available at `http://home.mit.bme.hu/~bank/thesis/index.html` .

[Bank 2003] Bank, B., Avanzini, F., Borin, G., De Poli, G., Fontana, F. and Rocchesso, D. "Physically informed signal-processing methods for piano sound synthesis: A research overview," *EURASIP J. Applied Signal Proc.*, vol. **2003**(10), 2003, pp. 941–952.

[Bank 2004] Bank, B. and Sujbert, L. "A piano model including longitudinal string vibrations," *Proc. Int. Conf. Dig. Audio Ef.*, 2004, pp. 89–94

[Benade 1976] Benade, A. H. (1976). *Fundamentals of Musical Acoustics*. New York: Oxford University Press.

[Bensa 2003] Bensa, J., Bilbao, S., Kronland-Martinet, R. and Smith, J. O. "The simulation of piano string vibration: From physical models to finite difference schemes and digital waveguides," *J. Acoust. Soc. Am.*, vol. **114**(2), 2003, pp. 1095–1107.

[Bensa 2004] Bensa, J., Jensen, K. and Kronland-Martinet, R. "A hybrid resynthesis model for hammer-string interaction of piano tones," *EURASIP J. Applied Signal Proc.*, vol. **2004**(7), 2004, pp. 1021–1035.

[Bilbao 2004a] Bilbao, S. "Parameterized families of finite difference schemes for the wave equation," Wiley Periodicals, Wilmington, DE, Numer. Methods Partial Differential Eq. (20), 2004, pp. 463–480.

[Bilbao 2004b] Bilbao, S. (2004). *Wave and Scattering Methods for the Numerical Integration of Partial Differential Equations*. PhD thesis, Stanford University, Stanford, CA. Available at `http://ccrma.stanford.edu/~bilbao/master/goodcopy.html` .

[Bilbao 2008] Bilbao, S. (2008). *Numerical Sound Synthesis*. Due for publication. Chichester, England, UK: John Wiley & Sons. Available as online book at `http://ccrma.stanford.edu/~bilbao/booktop/booktop.html` .

[Borin 1992] Borin, G., De Poli, G. and Sarti, A. "Sound Synthesis by Dynamic System Interaction." In D. Baggi (ed.) *Readings in Computer Generated Music*. Los Alamitos, CA: IEEE Computer Society Press. 1992, pp. 139–160.

[Borin 1996] Borin, G. and De Poli, G. "A hysteretic hammer-string interaction model for physical model synthesis," *Proc. Nord. Acoust. Meet.*, 1996, pp. 399–406.

[Borin 1997] Borin, G., Rocchesso, D. and Scalcon, F. "A physical piano model for music performance," *Proc. Int. Comput. Mus. Conf.*, 1997, pp. 350–353.

[Boutillon 1988] Boutillon, X. "Model for piano hammers: Experimental determination and digital simulation," *J. Acoust. Soc. Am.*, vol. **83**(2), 1988, pp. 746–754.

[Chaigne 1994a] Chaigne, A. and Askenfelt, A. "Numerical simulations of piano strings. I. A physical model for a struck string using finite difference methods," *J. Acoust. Soc. Am.*, vol. **95**(2), 1994, pp. 1112–1118.

[Chaigne 1994b] Chaigne, A. and Askenfelt, A. "Numerical simulations of piano strings. I. Comparisons with measurements and systematic exploration of some hammer-string parameters," *J. Acoust. Soc. Am.*, vol. **95**(3), 1994, pp. 1631–1640.

[Conklin 1996a] Conklin, H. A. "Design and tone in the mechanoacoustic piano. Part I. Piano hammers and tonal effects," *J. Acoust. Soc. Am.*, vol. **99**(6), 1996, pp. 3286–3296.

[Conklin 1996b] Conklin, H. A. "Design and tone in the mechanoacoustic piano. Part III. Piano strings and scale design," *J. Acoust. Soc. Am.*, vol. **100**(3), 1996, pp. 1286–1298.

[d'Alembert 1747] d'Alembert, J. le Rond. "Investigation of the curve formed by a vibrating string." In R. B. Lindsay (ed.) *Acoustics: Historical and Philosophical Development*. Stroudsburg, PA: Dowden, Hutchinson & Ross. 1973, pp. 119–123.

[Ducasse 2005] Ducasse, É. "On waveguide modelling of stiff piano strings," *J. Acoust. Soc. Am.*, vol. **118**(3), 2005, pp. 1776–1781.

[Fletcher 1998] Fletcher, N. H. and Rossing, T. D. (1998). *The Physics of Musical Instruments*. 2nd ed. New York: Springer.

[Garnett 1987] Garnett, G. E. "An approach to sound morphing based on physical modelling," *Proc. Int. Comput. Mus. Conf.*, 1987, pp. 89–95.

[Giordano 1997] Giordano, N. "Simple model of a piano soundboard," *J. Acoust. Soc. Am.*, vol. **102**(2), 1997, pp. 1159–1168.

[Hall 1988] Hall, D. E. and Askenfelt, A. "Piano string excitation V: Spectra for real hammers and strings," *J. Acoust. Soc. Am.*, vol. **83**(4), 1988, pp. 1627–1638.

[Hall 1990] Hall, D. E. (1990). *Musical Acoustics*. 2nd ed. Pacific Grove, CA: Brooks/Cole.

[Hall 1992] Hall, D. E. "Piano string excitation VI: Nonlinear modelling," *J. Acoust. Soc. Am.*, vol. **92**(1), 1992, pp. 95–105.

[Hikichi 1999] Hikichi, T. and Osaka, N. "An approach to sound morphing based on physical modelling," *Proc. Int. Comput. Mus. Conf.*, 1999, pp. 108–111.

[Hiller 1971a] Hiller, L. and Ruiz, P. "Synthesizing musical sounds by solving the wave equation for vibrating objects: Part 1," *J. Audio Eng. Soc.*, vol. **19**, 1971, pp. 462–470.

[Hiller 1971b] Hiller, L. and Ruiz, P. "Synthesizing musical sounds by solving the wave equation for vibrating objects: Part 2," *J. Audio Eng. Soc.*, vol. **19**, 1971, pp. 542–551.

[Hofstadter 2000] Hofstadter, D. R. (2000). *Gdel, Escher, Bach: an Eternal Golden Braid*. 20th-anniversary edn. London: Penguin Books.

[Jaffe 1983] Jaffe, D. A. and Smith, J. O. "Extensions of the Karplus-Strong plucked-string algorithm," *Comput. Music J.*, vol. **7**(2), 1983, pp. 56–69.

[Jaffe 1995] Jaffe, D. A. "Ten criteria for evaluating synthesis techniques," *Comput. Music J.*, vol. **19**, 1995, pp. 76–87.

[Järveläinen 1999] Järveläinen, H., Välimäki, V. and Karjalainen, M. "Audibility of inharmonicity in string instrument sounds, and implications to digital sound synthesis," *Proc. Int. Comput. Mus. Conf.*, 1999, pp. 359–362.

[Karjalainen 2004] Karjalainen, M. and Erkut, C. "Digital waveguides versus finite difference structures: Equivalence and mixed modelling," *EURASIP J. Applied Signal Proc.*, vol. **2004**(7), 2004, pp. 978–989.

[Karplus 1983] Karplus, K. and Strong, A. "Digital synthesis of plucked-string and drum timbres," *Comput. Music J.*, vol. **7**(2), 1983, pp. 43–55.

[Morse 1948] Morse, P. M. (1948). *Vibration and Sound*. 2nd edn. Columbus, OH: McGraw-Hill.

[Reinholdt 1987] Reinholdt, A., Jansson, E. and Askenfelt, A. "Analysis and synthesis of piano tone," *J. Acoust. Soc. Am.*, vol. **81**(S1), 1987, pp. S61.

[Rocchesso 1996] Rocchesso, D. and Scalcon, F. "Accurate dispersion simulation for piano strings," *Proc. Nordic Acoust. Meeting*, 1996, pp. 407–414.

[Rocchesso 1999] Rocchesso, D. and Scalcon, F. "Bandwidth of perceived inharmonicity for physical modelling of dispersive strings," *IEEE Trans. Speech Audio Proc.*, vol. **7**(5), 1999, pp. 597–601.

[Smith 1987] Smith, J. O. "Music applications of digital waveguides," CCRMA, Dept. Music, Stanford University, Stanford, CA, Tech. Rep. STAN-M-39, 1987.

[Smith 1992] Smith, J. O. "Physical modelling using digital waveguides," *Comput. Music J.*, vol. **16**(4), 1992, pp. 74–91.

[Smith 1995] Smith, J. O. and Van Duyne, S. A. "Commuted piano synthesis," *Proc. Int. Comput. Mus. Conf.*, 1995, pp. 335–342.

[Smith 2008] Smith, J.O. (2008). *Physical Audio Signal Processing*, May 2008 edn. Online book, available at `http://ccrma.stanford.edu/~jos/pasp/` .

[Stulov 1995] Stulov, A. "Hysteretic model of the grand piano hammer felt," *J. Acoust. Soc. Am.*, vol. **97**(4), 1995, pp. 2577–2585.

[Suzuki 1987] Suzuki, I. "Model analysis of a hammer-string interaction," *J. Acoust. Soc. Am.*, vol. **82**(4), 1987, pp. 1145–1151.

[Taflove 1995] Taflove, A. and Hagness, S. C. (1995). *Computational Electrodynamics: The Finite-Difference Time-Domain Method*. 2nd edn. Norwood, MA: Artech House.

[Thomas 1995] Thomas, J. W. (1995). *Numerical Partial Differential Equations: Finite Difference Methods*. New York: Springer-Verlag.

[Trautmann 2003] Trautmann, L. and Rabenstein, R. (2003). *Digital Sound Synthesis by Physical Modeling Using the Functional Transformation Method*. New York: Kluwer/Plenum.

[Van Duyne 1994a] Van Duyne, S. A. and Smith, J. O. "A simplified approach to modelling dispersion caused by stiffness in strings and plates," *Proc. Int. Comput. Mus. Conf.*, 1994, pp. 407–410.

[Van Duyne 1994b] Van Duyne, S. A. and Smith, J. O. "The Wave Digital Hammer: A computationally efficient traveling wave model of the piano hammer and the felt mallet," *J. Acoust. Soc. Am.*, vol. **96**(5), 1994, pp. 3300–3301.

[Van Duyne 1994c] Van Duyne, S. A. and Smith, J. O. "Travelling wave implementation of a lossless mode-coupling filter and the Wave Digital Hammer," *Proc. Int. Comput. Mus. Conf.*, 1994, pp. 411–418.

[Van Duyne 1995] Van Duyne, S. A. and Smith, J. O. "Developments for the commuted piano," *Proc. Int. Comput. Mus. Conf.*, 1995, pp. 319–326.

[Välimäki 1995] Välimäki, V. (1995). *Discrete-Time Modelling of Acoustic Tubes Using Fractional Delay Filters*. PhD thesis, Helsinki University of Technology, Espoo, Finland. Available at `http://www.acoustics.hut.fi/~vpv/publications/vesa_phd.html` .

[Välimäki 1996] Välimäki, V., Huopaniemi, J., Karjalainen, M. and Jánosy, Z. "Physical modelling of plucked string instruments with application to real-time sound synthesis," *J. Audio Eng. Soc.*, vol. **44**(5), 1996, pp. 331–353.

[Välimäki 2006] Välimäki, V., Pakarinen, J., Erkut, C. and Karjalainen, M. "Discrete-time modelling of musical instruments," IOP Publishing, Bristol, Rep. Prog. Phys. (69), 2006, pp. 1–78.

[Weinreich 1977] Weinreich, G. "Coupled piano strings," *J. Acoust. Soc. Am.*, vol. **62**(6), 1977, pp. 1474–1484.

[Yee 1966] Yee, K. S. "Numerical Solution of initial boundary value problems involving Maxwells equations in isotropic media" *IEEE Trans. Antennas Propagat.*, vol. **14**, 1966, pp. 302–307.